



# Characterising key bacterial taxa of the benthic diatom *Amphora* sp. biofilms in a porous substrate photobioreactor

Nadeeshani Dehel Gamage<sup>a,\*</sup>, Paul Délérís<sup>a</sup>, Leïla Tirichine<sup>b,c</sup>, Gaëtane Wielgosz-Collin<sup>a</sup>, Thierry Lebeau<sup>d</sup>, Aurélie Mossion<sup>a</sup>, Vona Méléder<sup>a,e</sup>

<sup>a</sup> Nantes Université, Institut des Substances et Organismes de la Mer, ISOMer, UR 2160, F-44000, Nantes, France

<sup>b</sup> Nantes Université, CNRS, Unité en Sciences Biologiques et Biotechnologies (US2B), UMR 6286, 2 rue de la Houssinière, 44322 Nantes, France

<sup>c</sup> Institute for Marine and Antarctic Studies (IMAS), Ecology and Biodiversity Centre, University of Tasmania, Hobart, TAS, 7004, Australia

<sup>d</sup> Nantes Université, Laboratoire de Planétologie et Géosciences, UMR LPG-Nantes 6112 CNRS, 2 rue de la Houssinière, BP, 92208, 44322, Nantes Cedex, France

<sup>e</sup> Institut universitaire de France (IUF), 103 Boulevard Saint-Michel, 75005, Paris, France

## ARTICLE INFO

### Keywords:

Bacterial temporal succession  
Benthic diatom biofilms  
Exponential-phase bacterial dynamics  
Mutualistic interactions  
Photobioreactor ecology

## ABSTRACT

Microalgae-bacteria interactions have recently emerged as a potential approach to enhance microalgal growth and metabolite production. However, successful co-culturing relies on synergistic and metabolically complementary interactions between microalgae and associated microorganisms, which enhance culture stability and productivity. Rather than introducing exogenous bacteria, characterising native host-associated microbiomes represents an ecologically relevant strategy, as these communities may reflect long-standing mutualistic or syntrophic interactions. Despite increasing interest in biofilm-based cultivation, microbial dynamics within microalgal biofilms in bioreactors remain poorly understood compared to planktonic systems. In this study, we investigated bacterial succession in a monoalgal biofilm of the oleaginous benthic diatom *Amphora* sp. during its exponential growth phase in a porous substrate photobioreactor (PSBR), aiming to identify key bacterial taxa for future co-culturing experiments. The exponential phase was targeted due to its relevance for biomass accumulation and active cellular metabolism underpinning productivity in biofilm-based systems. Non-axenic *Amphora* sp. was grown in F/2-enriched artificial seawater, and bacterial community dynamics were assessed at Day 0, Day 3 (mid-exponential), and Day 6 (late-exponential) using PacBio Sequel II/Ile 16S rRNA amplicon sequencing. Distinct phase-dependent shifts in bacterial community composition were observed, with Alphaproteobacteria declining over time and concomitant increases in Flavobacteriia and Planctomycetota. Despite these changes, bacterial communities maintained relatively stable evenness, structured around a few pivotal taxa. *Marivita*, *Sulfitobacter*, *Polaribacter*, and *Rhodopirellula* were identified as key bacterial taxa dynamically associated with the exponential phase of *Amphora* sp. Overall, this study provides a foundational screening framework to identify native bacterial candidates for co-culturing with mono-microalgal biofilms.

## 1. Introduction

Microalgae are versatile photosynthetic microorganisms increasingly explored as sources of high-value bioactive compounds for use in nutraceuticals, pharmaceuticals, food, and cosmetics, and for functional applications including bioenergy production, agricultural biostimulants, and wastewater treatment (Borowitzka, 2013; Yuan et al., 2021). Depending on the intended application and production scale, they are cultivated in either open systems (e.g., raceway ponds) or closed systems

(e.g., photobioreactors), each with distinct advantages and challenges related to cost, contamination risk, scalability, and environmental control (Fulbright et al., 2018). Conventionally, efforts in microalgae cultivation have focused on maintaining monocultures of strains to produce highly valuable metabolites such as lipids, pigments, and proteins (Moejes et al., 2017; Fulbright et al., 2018). However, maintaining axenic monocultures is often technically challenging and economically unsustainable, particularly at large scales (Vale et al., 2023). Contaminations, whether airborne, waterborne, or introduced during routine

\* Corresponding author.

E-mail addresses: [nadeeshani.dehel-gamage@univ-nantes.fr](mailto:nadeeshani.dehel-gamage@univ-nantes.fr) (N.D. Gamage), [Paul.Deleris@univ-nantes.fr](mailto:Paul.Deleris@univ-nantes.fr) (P. Délérís), [tirichine-l@univ-nantes.fr](mailto:tirichine-l@univ-nantes.fr) (L. Tirichine), [Gaetane.Wielgosz-Collin@univ-nantes.fr](mailto:Gaetane.Wielgosz-Collin@univ-nantes.fr) (G. Wielgosz-Collin), [thierry.lebeau@univ-nantes.fr](mailto:thierry.lebeau@univ-nantes.fr) (T. Lebeau), [Aurelie.Mossion@univ-nantes.fr](mailto:Aurelie.Mossion@univ-nantes.fr) (A. Mossion), [vona.meleder@univ-nantes.fr](mailto:vona.meleder@univ-nantes.fr) (V. Méléder).

<https://doi.org/10.1016/j.biteb.2026.102686>

Received 7 November 2025; Received in revised form 27 February 2026; Accepted 7 March 2026

Available online 10 March 2026

2589-014X/© 2026 The Author(s). Published by Elsevier Ltd. This is an open access article under the CC BY license (<http://creativecommons.org/licenses/by/4.0/>).

handling, can significantly disrupt the stability and productivity of microalgal production systems (Paquette et al., 2020; Steinrücken et al., 2023). In some cases, sudden culture crashes have been triggered by microbial competition, antagonism, or parasitism of algal strains, posing a serious obstacle to industrial-scale operations (Moejes et al., 2017; Fulbright et al., 2018; Davies et al., 2021; Aalto et al., 2024). Despite these challenges, recent studies have begun to highlight the potential benefits of incorporating natural or synthetic microbial communities into microalgal cultures, or co-culturing algal strains with their microbial associates (Cho et al., 2015; Wang et al., 2015; Molina-Cárdenas et al., 2020; Chorazyczewski et al., 2021; Sittmann et al., 2021; Bui-Xuan et al., 2022; Steinrücken et al., 2023). Instead of being viewed solely as contaminants, certain microorganisms, particularly bacteria, can form mutualistic or commensal relationships with microalgae, enhancing nutrient availability, promoting algal growth, improving stress tolerance, and increasing intracellular accumulation of target compounds of microalgae (Lakaniemi et al., 2012; Lopes et al., 2025). Consequently, microbiome engineering comes to play as an emerging, cost-effective, and environmentally sustainable strategy in microalgal biotechnology, with the potential to enhance the productivity by mimicking natural ecosystem dynamics (Lian et al., 2018; Kumar et al., 2020).

The success of microbiome engineering largely depends on the synergistic interactions and metabolic complementarity between microalgae and their microbial partners, which ultimately influence both culture stability and overall productivity (Aalto et al., 2024; Lopes et al., 2025). To achieve this, selecting bacterial partners based on their natural co-occurrence with specific microalgae would be an ideal and ecologically relevant strategy, as such associations often reflect mutualistic or syntrophic relationships that activate biosynthetic pathways for key target compounds (Krohn-Molt et al., 2017; Lopes et al., 2025). Several studies have demonstrated enhanced microalgal growth, biomass accumulation, and metabolite yields through the use of bacterial partners either isolated from the native microbiota of the microalgal host or via manipulation of the natural microbiome (Cho et al., 2015; Lépinay et al., 2018; Chorazyczewski et al., 2021). For example, co-culturing native bacteria with their microalgal hosts such as *Ankistrodesmus* sp. with *Rhizobium* sp. (Nascimento et al., 2013), *Scenedesmus obliquus* with *Acidovorax facilis* (Wang et al., 2015), and *Phaeodactylum tricornutum* with *Marinobacter* sp. (Chorazyczewski et al., 2021) has led to improved biomass and lipid yields in suspension cultures. Similarly, replacing the native microbiota of *Chlorella vulgaris* with a synthetic consortium assembled from selected native strains led to significantly higher biomass production than both its axenic and non-axenic counterparts (Cho et al., 2015). However, not all associations between microalgae and their native bacteria are beneficial. Chorazyczewski et al. (2021) reported culture crashes when *Phaeodactylum tricornutum* was co-cultivated with its native isolates *Algoriphagus* sp. and *Muricauda* sp., and in another study, we observed significant reductions in *Amphora* sp. biomass in binary co-cultures with native isolates, *Maribacter* sp., *Pseudomonas* sp., *Janibacter* sp., *Brevundimonas* sp., *Aureimonas* sp., and *Erythrobacter* sp. (Gamage et al., 2026a). Therefore, a fundamental understanding of bacterial dynamics, together with the selection of key native, host-associated microbial partners, represents essential steps toward effective microbiome engineering in microalgal biotechnology.

The composition and development of bacterial communities associated with microalgae are highly species-specific and are shaped by various factors, including geographical origin, availability of extracellular products in the phycosphere, culture medium composition, culture mode (open, indoor), long term maintenance or storage and the physiological state of the microalgal host (Moejes et al., 2017; Lépinay et al., 2018; Filho et al., 2021; Steinrücken et al., 2023). Variations in species richness and community composition have primarily been linked to changes in the availability of organic carbon fractions, including dissolved organic carbon released by microalgae, organic matter from senescent or lysed cells, and other metabolites within the phycosphere

(Grossart et al., 2005; Steinrücken et al., 2023; Lipsman et al., 2024). These compounds may exert selective pressure, promoting the development of adapted bacterial populations over the course of algal growth (Schäfer et al., 2002). Across temporal scales, studies investigating bacterial communities in suspended microalgal cultures have reported varying outcomes, reflecting the complex and dynamic nature of algae-bacteria interactions under different culture conditions. For instance, Moejes et al. (2017) observed marked shifts in bacterial community composition across the lag, exponential, stationary, and declining phases of *Phaeodactylum tricornutum* cultures grown over 22 days in different nutrient-rich media. In contrast, Lupette et al. (2016) found stable communities in *Ostreococcus tauri* cultures maintained for 35 days under different photoperiod and medium conditions, up to the declining phase. Furthermore, Steinrücken et al. (2023) also reported that bacterial communities remained relatively stable in batch cultures of three *Phaeodactylum* strains grown for 10 days in bubble columns, up to the stationary phase. However, most microbiome-related studies to date have focused on planktonic microalgae, while natural biofilms (e.g., freshwater and marine) have primarily been investigated from an environmental perspective (Pohlon et al., 2010; Xing et al., 2015; Pollet et al., 2018; Sushmitha et al., 2021).

Given the growing interest in biofilm-based microalgal culture systems as cost-effective alternatives to suspended cultures, owing to their higher harvesting efficiency and reduced water and energy demands (Yuan et al., 2021; Arnaldo et al., 2024), integrating microbiome engineering could also offer an innovative strategy for enhancing yield and metabolic productivity in microalgal biofilm systems (Gamage et al., 2026a). As microalgal biofilms naturally harbour diverse microorganisms, primarily bacteria, due to their rich extracellular polymeric substances (Vale et al., 2023), understanding microbial dynamics within these biofilms may facilitate the effective integration of suitable bacterial candidates to enhance their biotechnological potential. However, there is limited understanding of the bioreactor ecology of mono-microalgal biofilms, particularly the co-occurrence, composition, and temporal succession of associated bacterial taxa. To address this knowledge gap, this study aimed to (i) characterize the temporal succession of bacterial communities associated with the exponential growth phase of a biofilm-forming marine benthic diatom, *Amphora* sp., cultivated in a laboratory-scale vertical biofilm porous substrate photobioreactor (PSBR), and (ii) identify key bacterial taxa dynamically associated with this metabolically active phase as candidates for future co-culturing and microbiome engineering studies. The focus on the exponential growth phase was motivated by its importance for biomass accumulation and active cellular metabolism in microalgae, which underpin productivity in biofilm-based cultivation systems (Indrayani et al., 2020), compared to growth-limiting or stress-associated conditions during the stationary phase (Goto et al., 1999; Cointet et al., 2021). In this study, non-axenic *Amphora* sp. was pre-incubated for 4 days on filter discs to establish a biofilm, followed by transfer of the discs to a vertical biofilm PSBR for 6 days of cultivation. DNA was extracted at the end of the pre-incubation period (Day 0) and at the mid- (Day 3) and late-exponential (Day 6) phases of *Amphora* sp. grown in a PSBR and subsequently used for metabarcoding analysis. Consequently, the present study provides a foundational step toward identifying key native, host-selected bacterial taxa for designing defined algal-bacterial biofilm co-cultures.

## 2. Materials and methods

### 2.1. Non-axenic *Amphora* sp. culture maintenance

The stock culture of non-axenic *Amphora* sp. was maintained in 250 mL flasks containing artificial seawater (ASW) with a salinity of 28 ‰ and a pH of 7.8, enriched with F/2 medium (see Supplementary I), and incubated at 16 °C under a 12:12 h light-dark cycle with a light intensity of 100 µmol photons·m<sup>-2</sup>·s<sup>-1</sup>. This strain was originally isolated from

the northwest coast of France (47°22'06" N, 02°32'52" W) and maintained under the code NCC169 in the Nantes Culture Collection (NCC) at the ISOMer laboratory, Nantes University. It is now archived in the Roscoff Culture Collection (RCC) under accession number RCC5813.

## 2.2. Cultivation of non-axenic *Amphora* sp. in the biofilm PSBR

The cultivation of non-axenic *Amphora* sp. in the vertical PSBR system involved inoculating filter discs, followed by the initiation of the PSBR operation. The customized PSBR (based on the Nano model by Synoxis Algae, France), designed for microalgal biofilm cultivation, is described in detail by Arnaldo et al. (2024). For disc inoculation, microfiber filters (Ø 25 mm, 1.2 µm pore size, Whatman™ GF/C, China) were used as growth substrates. To establish a stable biofilm of non-axenic *Amphora* sp. on these filters, a 4-day pre-incubation was carried out outside the PSBR. This step was necessary as direct introduction of freshly inoculated discs into the vertical PSBR would result in cell washout due to periodic nutrient flow. Thus, pre-combusted (at 400 °C for 4 h) and pre-weighed discs were inoculated with  $2 \times 10^6$  cells (counted using a Neubauer hemocytometer under 40× magnification) in 2 mL of enriched ASW and placed in 6-well tissue culture plates (Dutscher, China). The plates were incubated at  $18 \pm 1$  °C under continuous white light ( $100 \mu\text{mol photons}\cdot\text{m}^{-2}\cdot\text{s}^{-1}$ ) under aseptic conditions. A total of 30 discs were prepared for each of the three trials (i.e., 90 discs in total). Following incubation, the discs were mounted onto the PSBR's metal plate, which had been wrapped in a thin layer of tissue paper to facilitate adhesion through capillary action. The metal plate with the attached discs was then transferred into the growth chamber of the sterilized PSBR. Prior to assembly, all PSBR components including the PMMA chambers, nutrient sparger, connecting valves, and tubing were sterilized according to the manufacturer's protocol. Calibration of the pH probe and dosing pumps was performed before each run. Light intensity inside the PSBR was maintained at  $100 \mu\text{mol photons}\cdot\text{m}^{-2}\cdot\text{s}^{-1}$ , using a blend of 25% green (~520 nm), 25% red (~630 nm and 660 nm), and 27% blue light (~450 nm). The reservoir chamber was filled with 700 mL of culture medium. This medium was delivered through a nutrient sparger positioned above the metal disc holder at a rate of 1 mL every 5 min, while the used medium in the growth chamber was recirculated back to the reservoir at a rate of 8 mL every 5 min. The entire system operated at a controlled room temperature of  $18 \pm 1$  °C. The experiment was conducted in triplicate, with each run lasting 6 days in batch mode. Furthermore, non-axenic *Amphora* sp. cultures were intentionally used in this study to characterize naturally assembled, host-associated bacterial communities under PSBR conditions, with the aim of identifying native key bacterial taxa associated with the exponential growth phase of *Amphora* sp., thus, axenic conditions were not employed. As key bacterial taxa were identified based on defined selection criteria (see Section 2.5), including reproducible detection across biological replicates, these taxa were considered to be consistently associated with the host biofilm rather than resulting from random background colonization.

## 2.3. Discs harvesting and DNA extraction of microbiome

Based on the growth analysis of non-axenic *Amphora* sp. in the biofilm PSBR over 15 days under the same conditions described above, the exponential phase was found to last for approximately 7 days from the start of the PSBR run (Gamage et al., 2026b). However, the transition from lag to exponential phase could not be detected due to the 4-day pre-incubation period outside the PSBR. Therefore, DNA extractions of the microbiome associated with *Amphora* sp. were performed on Day 0 (end of disc pre-incubation), Day 3 (mid-exponential phase), and Day 6 (late-exponential phase). At each time point, 10 discs were randomly harvested from each trial and pooled into a 50 mL Falcon tube with 10 mL of sterilized enriched ASW. In total, nine pooled samples were obtained across three trials and three time points. The samples were vortexed for

30 s, followed by centrifugation at 1500g for 20 min at 4 °C. Supernatant was carefully removed and the total DNA was extracted using the NucleoSpin Microbial DNA Mini Kit (Macherey-Nagel, Germany) according to the manufacturer's instructions. DNA quantity and quality were estimated the optical density (OD) measurements at 260 nm and 280 nm ( $\text{OD}_{260\text{nm}}/\text{OD}_{280\text{nm}} = 1.8\text{--}2.2$ , Sambrook and Russell, 2001) using SkanIt microplate reader software (version 7.0.2.5) and a Varioskan Lux spectrophotometer with a µDrop plate (Thermo Fisher Scientific™, France). The extracted DNA samples from each time point were then sent to the service provider (Novogene, UK) for sequencing using the PacBio Sequel II/IIe.

## 2.4. Microbiome and bioinformatic analysis

Bacterial 16S rRNA genes were amplified for their V3 - V4 hyper-variable region using the primer pair 341f (CCTAYGGGRBGCASCAG) and 806r (GGACTACNNGGTATCTAAT). Amplified DNA fragments were end-repaired, A-tailed, and ligated with adapters to construct a SMRTbell library using AMPure PB beads for purification. Sequencing primers and polymerase were bound to the templates, and the library was quantified with Qubit before pooling and sequencing on the PacBio Sequel II/IIe (Novogene, UK). Sequencing generated between 45,236 and 55,443 high-quality (clean) reads per sample, with an average read length ranging from 1399 to 1458 bp, and total base counts per sample ranging from approximately 65.9 million to 80.3 million bases (see Supplementary II). The raw PacBio BAM files were demultiplexed by barcode to assign reads to their respective samples. These reads were then quality-filtered and processed to generate amplicon sequence variants (ASVs) and taxonomic annotation. Unlike operational taxonomic units (OTUs), which are commonly used in microbial studies and cluster sequences at a 97% similarity threshold, ASVs resolve single-nucleotide differences, providing greater accuracy and reproducibility (Callahan et al., 2017), therefore, ASVs were used in this study.

Denosing (excluding chimeric sequences), diversity analyses (after removing mitochondrial and chloroplast sequences), and differential abundance testing using analysis of composition of microbiomes (ANCOM) were performed in QIIME2 (version 2022.3). Sequences with fewer than five reads were discarded to construct the final ASV and feature tables. To account for differences in sequencing depth among samples, rarefaction analysis was performed based on ASV counts. Rarefaction curves for observed ASVs were generated to assess sequencing depth adequacy. Based on curve saturation, samples were rarefied to a common sequencing depth of 21,897 reads per sample prior to downstream alpha and beta diversity analyses. Rarefaction curves based on ASVs are provided in Supplementary III. Taxonomic classification of ASVs was carried out using the classify-sklearn plugin in QIIME2. Based on ASV annotations and feature tables, species abundance tables were generated across multiple taxonomic levels, from kingdom to species forming the core of the amplicon analysis. Further, a phylogenetic tree was constructed to represent the evolutionary relationships among ASVs. These outputs served as the foundation for downstream microbial community analyses, including the calculation of alpha diversity to assess within-sample diversity while beta diversity metrics were used to assess between-sample variations. The overall functional prediction of bacterial communities over time was performed using PICRUST2 based on ASVs derived from 16S rRNA sequencing. Gene family abundances were inferred by placing ASVs into the Greengenes reference phylogeny, and the functional spectra of both ancestral lineages and unclassified species were deduced. These were used to construct a functional prediction spectrum covering the domain of Bacteria. The bacterial community composition obtained from sequencing was then mapped onto this spectrum to predict metabolic functions, which were subsequently annotated using the Clusters of Orthologous Groups (COG) and Kyoto Encyclopedia of Genes and Genomes (KEGG) databases.



## 2.5. Statistics

Significant differences in the bacterial community composition associated with *Amphora* sp. in the biofilm-based PSBR system across Day 0, Day 3, and Day 6 were evaluated. The Kruskal-Wallis test with Dunn's post hoc analysis was used to assess significant changes across multiple taxonomic levels (phylum to species) over time, and the results were visualized in heatmaps based on z-scores of ASV relative abundances (Eq. (1)). To assess the diversity of bacterial communities within individual samples, alpha diversity metrics including Good's coverage (Good, 1953), richness (observed ASVs), Shannon's index, and Simpson's index (Kers and Saccenti, 2022) were calculated. Goods coverage was used to estimate sequencing depth, with higher values indicating higher the sequencing coverage (Eq. (2)). Richness represents the number of unique ASVs in a sample, higher values indicate greater richness (Eq. (3)). The Shannon's index indicates the total number of categories in the sample and their proportions. The higher the community diversity, the more uniform species distribution, and the greater the Shannon's index (Eq. (4)). The Simpson's index emphasizes the diversity and uniformity of species distribution in the community. The better the species uniformity, the greater the Simpson index (Eq. (5)). Significant differences in alpha diversity metrics across time points were tested using the Kruskal-Wallis Dunn's post hoc test. For beta diversity analysis, which measures the differences in bacterial community composition among samples, UniFrac distances (both weighted and unweighted) were calculated. Unweighted UniFrac considers only the presence or absence of taxa (Lozupone and Knight, 2005; Chen et al., 2012) (Eq. (6)) whereas weighted UniFrac incorporates both their relative abundance and presence or absence (Lozupone and Knight, 2008) (Eq. (7)). To visualize both inter-group and intra-group differences, non-metric multidimensional scaling (NMDS) based on weighted and unweighted UniFrac distances was performed using the *ade4* and *ggplot2* packages in R. Based on the abundance profiles obtained from functional annotations in the COG and KEGG databases, principal component analysis (PCA) was performed to visualize differences in functional composition among different harvesting days. Linear discriminant analysis effect size (LEfSe) was conducted using the LEfSe software to identify species with significant differences between groups, with the linear discriminant analysis (LDA). Dissimilarities and similarities in bacterial community composition within and between groups over time were assessed using ADONIS (PERMANOVA) and ANOSIM, based on the weighted UniFrac distance matrix. Key bacterial taxa were identified based on a combination of: (i) significant differential enrichment across time points determined by LEfSe analysis (LDA score > 4) (ii) substantial relative abundance during at least one exponential sub-phase and (iii) reproducible detection across biological replicates. *p*-Values < 0.05 were considered significantly different.

$$Z \text{ score} = \frac{ASV - \mu ASV}{SD} \quad (1)$$

$$\text{Good's coverage} = 1 - \frac{n1}{N} \quad (2)$$

$$\text{Richness (Observed ASVs)} = \sum_{s>0} 1_s \quad (3)$$

$$\text{Shannon's index} = - \sum_{i=1}^s p_i \log(p_i) \quad (4)$$

$$\text{Simpson's index} = \frac{1}{\sum_{i=1}^s p_i^2} \quad (5)$$

$$\text{Unweighted UniFrac distance} = \sum_{i=1}^n \frac{b_i |I(p_i^A > 0) - I(p_i^B > 0)|}{\sum_{i=1}^n b_i} \quad (6)$$

$$\text{Weighted uniFrac distance} = \sum_{i=1}^n b_i \times \left| \frac{A_i}{A_T} - \frac{B_i}{B_T} \right| \quad (7)$$

where ASV - the relative abundance of a taxon on a given day,  $\mu$ ASV - the mean abundance of that taxon across all sampling days, SD - the standard deviation,  $n1$  - the number of singleton ASVs (observed only once),  $N$  - the total number of sequences,  $s$  - the number of ASV,  $p_i$  - the proportion of the community represented by the  $i^{\text{th}}$  ASV,  $n$  - the total number of branches in the tree,  $b_i$  - the length of branch  $i$ ,  $A_i$  and  $B_i$  - the numbers of sequences that descend from branch  $i$  in communities A and B respectively, and  $A_T$  and  $B_T$  as the total numbers of sequences in communities A and B, respectively,  $p_i^A$  and  $p_i^B$  are the taxa proportions descending from the branch  $i$  for community A and B, respectively.

## 3. Results

### 3.1. Bacterial community composition

The bacterial community composition associated with non-axenic *Amphora* sp. across different taxonomic levels (phylum, class, family, and genus) in the biofilm PSBR at Days 0, 3, and 6 is shown in Fig. 1. On Day 0, Proteobacteria was the most significantly abundant phylum ( $p < 0.05$ , Dunn's post hoc test), accounting for 85.7% of the community. Its relative abundance declined over time. By Day 6, Bacteroidota and Planctomycetota had increased significantly compared to Day 0 and Day 3 ( $p < 0.05$ , Dunn's post hoc test), reaching 48.7% and 5.5%, respectively (Fig. 1a).

At the class level (Fig. 1b), Alphaproteobacteria and Acidimicrobiia were significantly more abundant classes on Day 0 ( $p < 0.05$ , Dunn's post hoc test) compared to Day 3 and Day 6, but their abundance declined over time. Among these, Alphaproteobacteria accounted for 80.6% of the total community on Day 0. Although Gammaproteobacteria, Saccharimonadia, Clostridia, and Bacilli tended to show higher relative abundances on Day 3 compared to other classes, the differences were not statistically significant ( $p > 0.05$ , Dunn's post hoc test), and their proportions declined by Day 6. All other classes exhibited a gradual increase in abundance over time, with Bacteroidia and Planctomycetes showing significant increases ( $p < 0.05$ , Dunn's post hoc test), reaching 48.0% and 5.4%, respectively.

The most abundant bacterial families recorded on Day 0 were Crocinitomicaceae, Marinobacteraceae, Rhodobacteraceae, Methylophilaceae, Ilumatobacteraceae, and Parvibaculaceae, along with moderate levels of Alcaligenaceae, Propionibacteriaceae and Solimonadaceae (Fig. 1c). Among these, Rhodobacteraceae and Parvibaculaceae exhibited significant abundance compared to other days ( $p < 0.05$ , Dunn's post hoc test), accounting for 73.8% and 1.3% of the total community, respectively. However, these major families showed a continuous decline in abundance over time, while the moderately abundant families initially decreased by Day 3 but returned to intermediate levels later. By Day 6, the three highly abundant families Flavobacteriaceae, Pirellulaceae, and Cyclobacteriaceae showed a significant increase ( $p < 0.05$ , Dunn's post hoc test).

Considering the top 30 genera based on abundance (Fig. 1d), *Winogradskyella*, *Marivita*, and *Phaeomarinobacter* were significantly more abundant on Day 0 than other days ( $p < 0.05$ , Dunn's post hoc test). Of these, *Marivita* accounted for approximately 72.2% of the total community. The abundance of *Sulfitobacter* and *Oceanibulbus* were significantly higher on Day 3 ( $p < 0.05$ , Dunn's post hoc test), accounting for 9.1% and 0.6%, respectively. But, while *Sulfitobacter* declined by Day 6, and *Oceanibulbus* remain significantly highly represented. By Day 6, the relative abundances of *Nitratireductor*, *Polaribacter*, *Oceanibulbus*, *Erythrobacter*, *Arenibacter*, *Rhodopirellula*, and *Pusillimonas* increased significantly ( $p < 0.05$ , Dunn's post hoc test) compared to Day 0 and Day 3. In this set, *Polaribacter* exhibited the highest relative abundance, accounting for 41.1% of the total community.

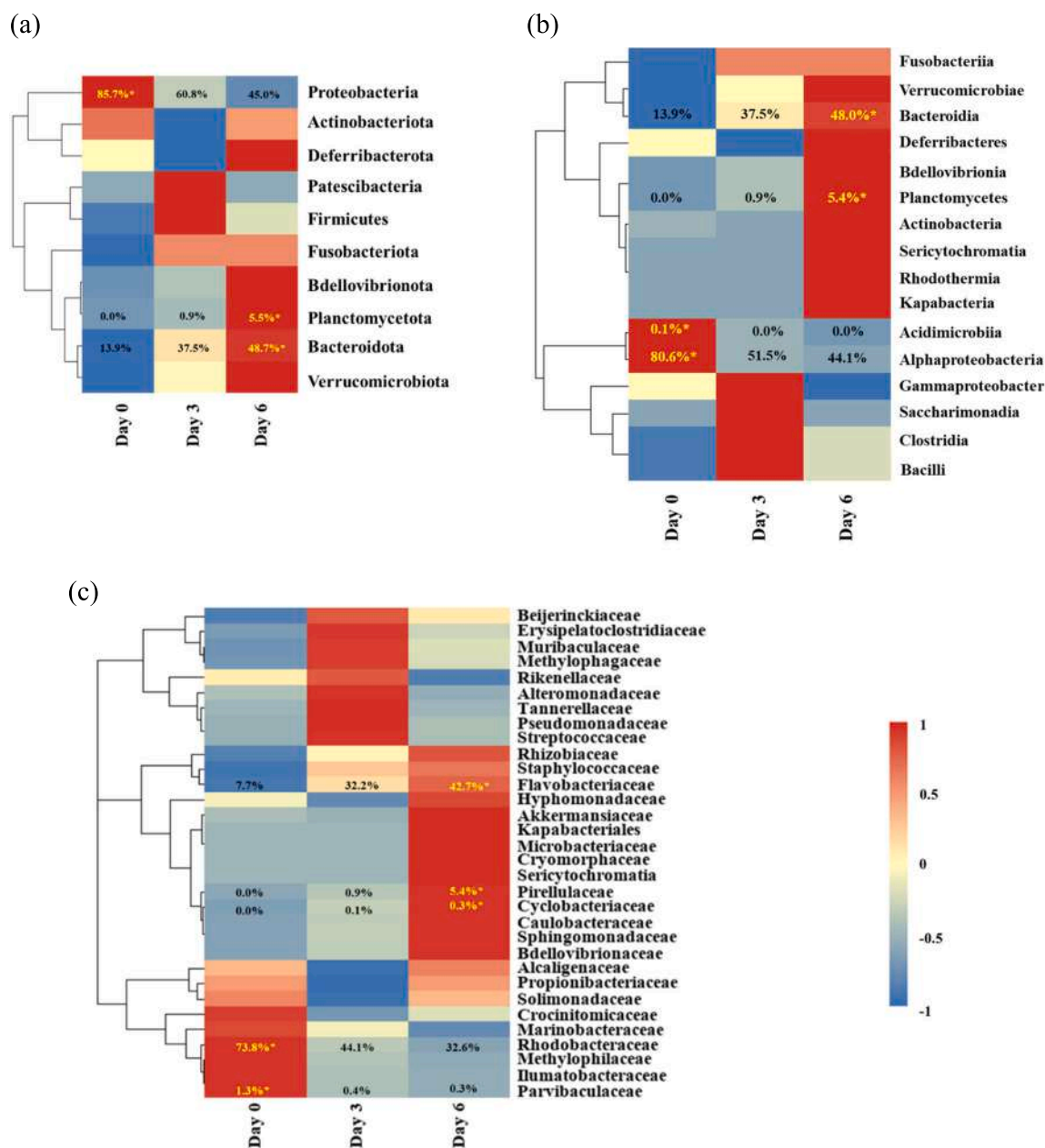


**Fig. 1.** Z-score-based heatmap showing the relative abundance of bacterial taxa associated with non-axenic *Amphora* sp. in the biofilm PSBR during the exponential phase, sampled at Day 0 (end of the pre-incubation of discs), Day 3 (mid-exponential phase), and Day 6 (late-exponential phase). (a) Phylum, (b) Class, (c) Family, and (d) Top 30 most abundant genera.  $n = 3$  per harvesting day. \* indicates a significant change in the abundance of a given taxon compared to other days (Kruskal-Wallis with Dunn's post hoc test,  $p$ -value  $< 0.05$ ). Temporal changes in average relative abundance percentage values of significantly changed taxa are shown inside the corresponding cells at Days 0, 3, and 6.

### 3.2. ASV composition dynamics

Microbiome analysis of *Amphora* sp. in the biofilm-based PSBR revealed a total of 200 bacterial ASVs, with 62 observed at Day 0, 121 at Day 3, and 145 at Day 6 (Fig. 2, see Supplementary IV). Among these, 41 ASVs were common to all three time points. Day 0 had 16 unique ASVs, while Day 3 and Day 6 exhibited greater microbial richness with 37 and 60 unique ASVs, respectively. Additionally, Day 3 shared 2 ASVs exclusively with Day 0 and 41 with Day 6, whereas Day 0 and Day 6 shared 3 ASVs not found on Day 3.

### 3.3. Differential analysis of alpha diversity indices

Alpha diversity analysis of bacterial communities associated with *Amphora* sp. in the PSBR is presented in Table 1. Sequencing depth was consistently sufficient across all time points, as indicated by a Good's coverage value of 1. The number of observed ASVs, reflecting species richness, increased significantly from  $54 \pm 16$  on Day 0 to  $80 \pm 11$  on Day 3, and  $98 \pm 29$  on Day 6 ( $p < 0.05$ , Dunn's post hoc test). This increase in richness was accompanied by a rise in Shannon diversity, which grew from  $2.63 \pm 0.18$  on Day 0 to  $2.98 \pm 0.47$  on Day 3, reaching  $3.06 \pm 0.14$  on Day 6, with a significant difference observed between Day 0 and Day 6 ( $p < 0.05$ , Dunn's post hoc test). In contrast, Simpson's index remained relatively stable over time, showing no

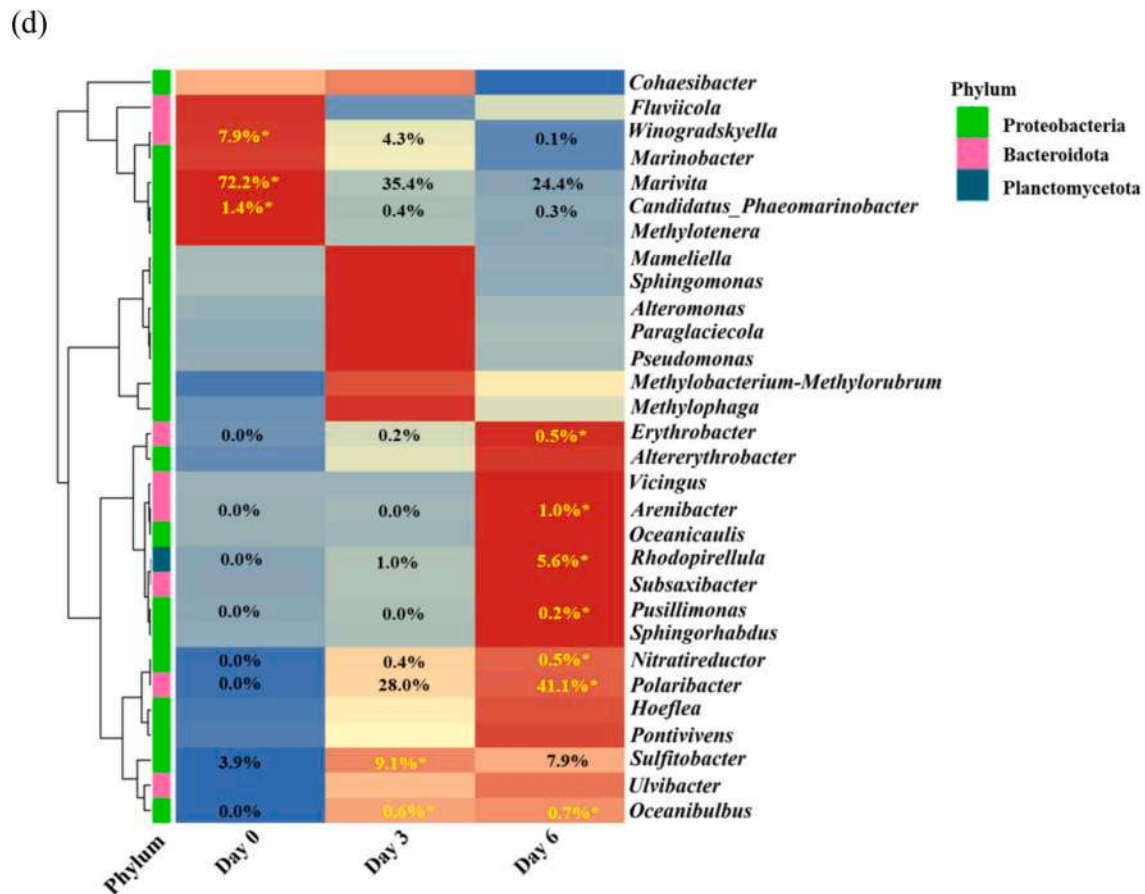


**Fig. 1.** (continued).

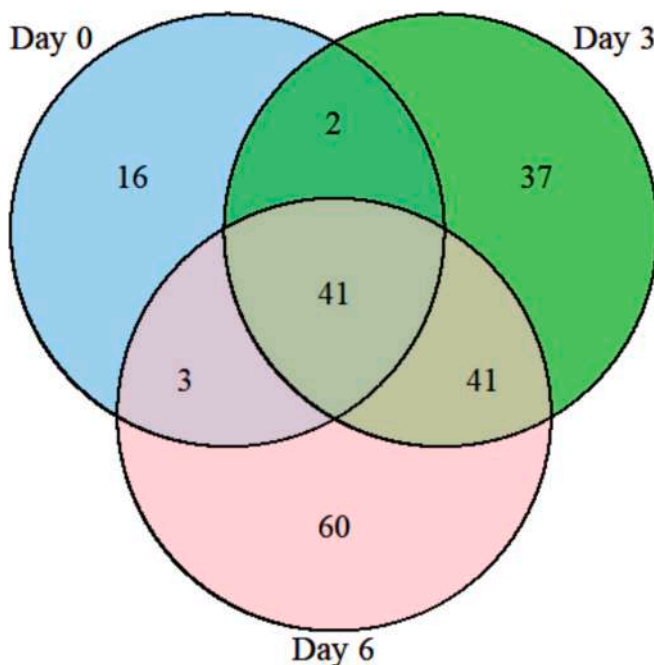


**Fig. 2.** Venn diagram illustrating the distribution of bacterial amplicon sequence variants (ASVs) associated with *Amphora* sp. during the exponential phase in biofilm PSBR, sampled at Day 0 (end of the pre-incubation of discs), Day 3 (mid-exponential phase), and Day 6 (late-exponential phase).  $n = 3$  per harvesting day.

Table 1

Alpha diversity metrics of bacterial communities associated with *Amphora* sp. during the exponential phase in the biofilm PSBR, sampled at Day 0 (end of the pre-incubation of discs), Day 3 (mid-exponential phase), and Day 6 (late-exponential phase).

Day	Goods coverage	Richness/Observed ASVs	Shannon	Simpson
Day 0	1 ± 0	54 ± 16 <sup>a</sup>	2.63 ± 0.18 <sup>a</sup>	0.74 ± 0.05 <sup>a</sup>
Day 3	1 ± 0	80 ± 11 <sup>b</sup>	2.98 ± 0.47 <sup>ab</sup>	0.73 ± 0.08 <sup>a</sup>
Day 6	1 ± 0	98 ± 29 <sup>b</sup>	3.06 ± 0.14 <sup>b</sup>	0.75 ± 0.02 <sup>a</sup>

Different superscript letters indicate statistically significant differences between sampling days for each alpha diversity metric ( $p < 0.05$ ). Values sharing the same letter are not significantly different.

significant changes in the bacterial community throughout the culture period  $p > 0.05$ , Dunn's post hoc test).

### 3.4. Beta diversity of bacterial dynamics across time

NMDS analysis based on UniFrac distances revealed temporal shifts in the bacterial community structure associated with exponential phase of *Amphora* sp. in the PSBR (Fig. 3). In the weighted UniFrac NMDS plot (Fig. 3a), which accounts for both the presence and relative abundance of taxa, Day 0 samples formed a clearly distinct cluster, separated from the later stages, while Day 3 and Day 6 samples showed substantial overlap. The low stress value (0.013) further indicates a high degree of reliability in the two-dimensional ordination. In contrast, the un-weighted UniFrac NMDS plot (Fig. 3b), which is based on the presence

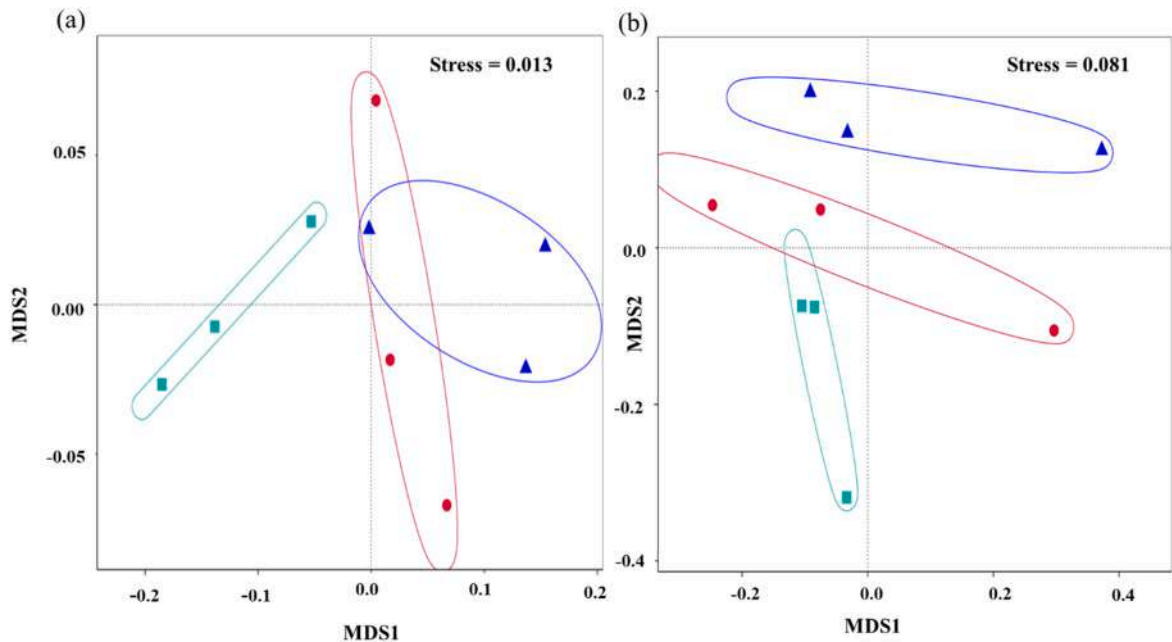


**Fig. 3.** Non-metric multi-dimensional scaling analysis (NMDS), (■) - Day 0 (end of the pre-incubation of discs), (●) - Day 3 (mid-exponential phase), (▲) - Day 6 (late-exponential phase) (a) NMDS based on weighted UniFrac distances (b) NMDS based on unweighted UniFrac distances. n = 3 per harvesting day. Stress level indicates the how well the multidimensional data are represented in the reduced two-dimensional (2D) space, stress < 0.05 indicates an excellent fit, <0.10 a good fit, <0.20 a fair but usable fit, >0.20 a poor fit, and >0.30 a highly suspect and unreliable ordination (Dexter et al., 2018).

or absence of taxa, showed well-defined separation among Day 0, Day 3, and Day 6 samples, with only minimal overlap between Day 0 and Day 3. The stress value (0.081) was within acceptable limits, supporting a good fit of the ordination.

3.5. Beta group significance tests

Statistical analysis using both ADONIS (PERMANOVA) and ANOSIM based on weighted UniFrac distances revealed significant temporal differences in the bacterial community structure associated with *Amphora* sp. in the PSBR (Table 2). The ADONIS (PERMANOVA) test revealed a significant temporal effect on bacterial community composition, with an  $R^2$  value of 0.65 ( $p$ -value = 0.012), indicating that 65% of the variation was attributable to differences among time points. Similarly, the ANOSIM test also supported significant temporal differences in bacterial communities, with an  $R$  value of 0.70 ( $p$ -value = 0.009), indicating that dissimilarities between time points were substantially greater than those within each time point. Together, these results indicate that the bacterial community composition changed significantly over time, reflecting a clear temporal shift in both the presence and relative abundance of bacterial taxa.

3.6. Key bacterial taxa from LEfSe analysis

LEfSe analysis identified statistically significant bacterial taxa associated with different stages of the exponential growth phase of *Amphora* biofilm (Fig. 4). At Day 0, the bacterial community was dominated by

*Marivita* and other Rhodobacteraceae lineages, identifying them as early colonizers. By Day 3, discriminative taxa shifted toward *Polaribacter* and *Sulfitobacter*, indicating a transitional stage marked by the enrichment of Flavobacteriia. At Day 6, the community was dominated by *Polaribacter* and *Rhodopirellula*, reflecting a late-exponential phase characterized by Flavobacteriia and Planctomycetota.

3.7. Phylogenetic relationship among bacterial taxa associated with *Amphora* sp.

Cladograms (Fig. 5) reveal the dynamic changes in bacterial community composition associated with *Amphora* sp. over time in the biofilm PSBR. At Day 0 (Fig. 5a and b), the bacterial community was largely enriched with members of the phylum Proteobacteria, while the phylum Actinobacteriota also made a significant contribution. Within Proteobacteria, the family Rhodobacteriaceae was predominant, whereas Ilumatobacteraceae represented a major taxonomic group within Actinobacteriota. By Day 3 (Fig. 5a) and Day 6 (Fig. 5b), the family Flavobacteriaceae within the phylum Bacteroidota played a significant role in the bacterial community. Additionally, at Day 6, Pirellulaceae and Xanthobacteraceae, belonging to the phyla Planctomycetota and Proteobacteria, respectively, also exhibited significant contributions, although their abundance was relatively low.

3.8. Functional diversity prediction

PCA plots illustrate the temporal dynamics of predicted functional

**Table 2**  
Statistical tests of temporal shifts in bacterial community composition during the exponential phase of *Amphora* sp. in the biofilm PSBR, based on weighted UniFrac distances.

Test	Distance metric	Test for	Statistic	p-Value
ADONIS (PERMANOVA)	Weighted UniFrac distance	Dissimilarities of bacterial composition between Vs within over time	$R^2 = 0.65$	0.012
ANOSIM	Weighted UniFrac distance	Similarity of bacterial communities within Vs between-groups over time	$R = 0.70$	0.009

ADONIS -  $R^2$  close to 1 means strong dissimilarity between groups.  
ANOSIM -  $R = 1 \rightarrow$  greater dissimilarity between groups,  $R = 0 \rightarrow$  even distribution within and between groups,  $R = -1 \rightarrow$  greater dissimilarity within groups.



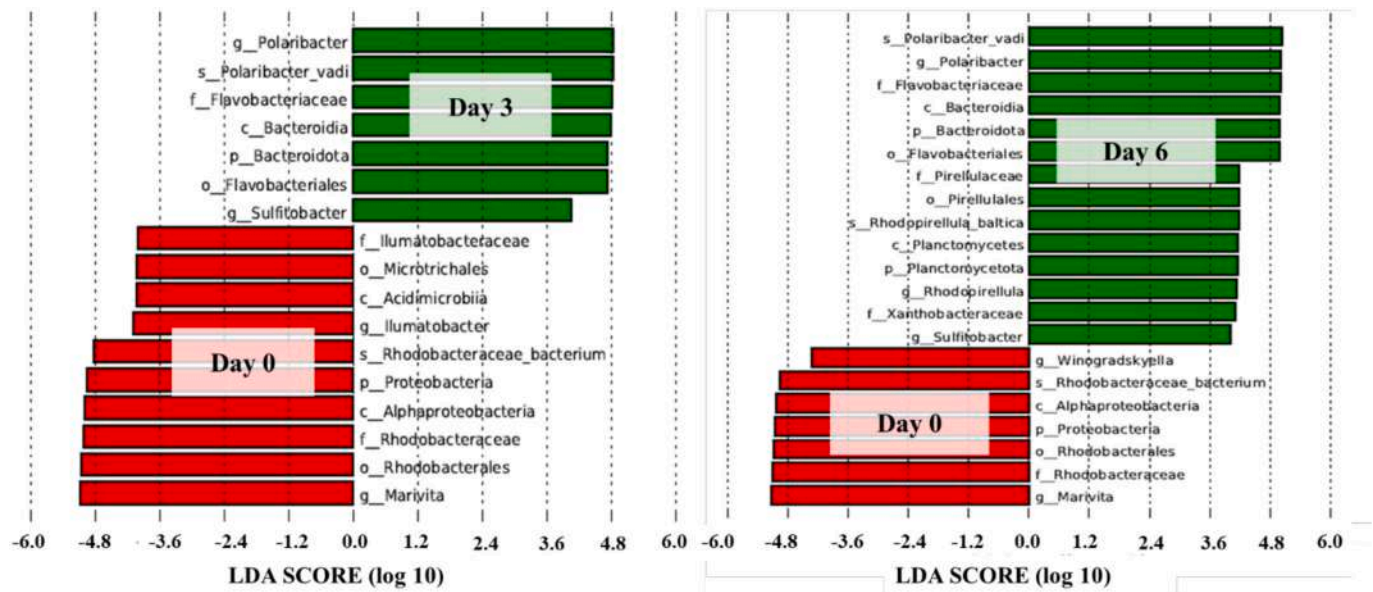


**Fig. 4.** Statistically significant biomarker taxa identified during the exponential phase of *Amphora* sp. biofilms, sampled at Day 0 (end of pre-incubation of discs), Day 3 (mid-exponential phase), and Day 6 (late-exponential phase), using LEfSe analysis.  $n = 3$  per harvesting day. Bacterial taxa with linear discriminant analysis (LDA) score greater than 4 are displayed.

pathway profiles in the bacterial community associated with *Amphora* sp. in the biofilm PSBR across three time points (Fig. 6). In the COG-based PCA (Fig. 6a), Day 0 samples form a tight and distinct cluster on the far-left side of the plot, reflecting a uniform and unique functional profile at the start of the PSBR experiment. By Day 3, samples shift markedly along PC1 and PC2 and display considerable variability, indicating a transitional phase with high intra-group heterogeneity in community functions. Day 6 samples form a compact and distinct cluster, positioned away from Day 0 and overlapping partially with Day 3, suggesting that the bacterial community had stabilized by the late exponential phase while retaining functional traces of the mid-phase transition. Similarly, the KEGG-based PCA (Fig. 6b) supported these observations, with Day 0 samples forming a tight cluster, Day 3 samples showing broad dispersion and overlapping with Day 6 samples, indicative of functional convergence. Taken together, the data reflect a major shift in predicted microbial functions from Day 0 to Day 3, followed by partial stabilization and functional convergence between Day 3 and Day 6.

#### 4. Discussion

Microalgal biofilms comprise complex, diverse communities whose composition and structure shift dynamically over time in response to host microalgal physiology, culture system (open or close) and environmental drivers (nutrient limitation, light intensity, shear stress, seasonal changes) (Grossart et al., 2005; Behringer et al., 2018; Schmidt et al., 2018; Aalto et al., 2024). In these systems, bacteria establish mainly through horizontal transmission via chemotaxis and extracellular polymetric substances interactions, or through vertical transmission where core microbiome members are inherited across algal subcultures (Pathom-aree et al., 2024). Unlike random transient encounters, leveraging these native bacteria enables the formation of stable mutualistic or syntrophic consortia with long-term persistence and functional interactions for biotechnological applications (Lopes et al., 2025). Thus, studying native bacterial dynamics elucidates how these communities assemble and evolve over time, revealing interaction networks, and functional roles (e.g., nutrient cycling and signalling) thereby supporting the identification of bacteria that enhance microalgal biofilm productivity or can be harnessed to construct mutualistic or

syntrophic consortia (Zhang et al., 2021; Pushpakumara et al., 2023). In this study, we provide an initial screening framework for identifying suitable host-associated bacterial taxa in microalgal biofilms using the natural biofilm-forming benthic diatom *Amphora* sp. grown in a PSBR.

Our results showed that bacterial species richness associated with *Amphora* sp. increased over time, as reflected by a rise in observed ASVs, consistent with findings in planktonic monoalgal cultures reported by Lupette et al. (2016), Moejes et al. (2017), Behringer et al. (2018), and Steinrücken et al. (2023). This trend was further supported by a rise in the Shannon index, which reflects both richness and evenness, suggesting that by the late exponential phase the community was not only richer in taxa but also more evenly structured. These dynamics could be mainly related to the increasing organic carbon fractions, such as dissolved organic carbon released by *Amphora* sp. and dissolved organic matter from senescent or lysed cells from both the diatom and associated bacteria, along with other metabolites present in the phycosphere (Sapp et al., 2007; Grossart et al., 2005; Steinrücken et al., 2023). On the other hand, Simpson's index showed that the microbiomes associated with *Amphora* sp. maintained stable evenness, with no single taxon becoming dominant, indicating that ecological balance and functional stability were preserved despite taxonomic turnover (Behringer et al., 2018). Such resilience could arise from functional redundancy, where multiple bacterial taxa perform overlapping ecological roles, thereby buffering the community against instability (Krohn-Molt et al., 2017).

In line with our study, Proteobacteria dominated the early *Amphora* sp. biofilm but declined over time, coinciding with a rise in Bacteroidota and a smaller yet noteworthy contribution from Planctomycetota. Similar succession patterns, with Proteobacteria as early colonizers and Bacteroidota together with low-abundance Planctomycetota as later dominant groups, have been reported in marine biofilms (Sushmitha et al., 2021). In contrast, Bacteroidetes appeared as early colonizers in freshwater biofilms, followed by Actinobacteria and Proteobacteria in later stages (Pohlson et al., 2010). Likewise, Grossart et al. (2005) found Bacteroidota to be dominant in biofilms associated with the marine diatom, *Thalassiosira rotula* during both exponential and stationary phases. Within Proteobacteria, Alphaproteobacteria showed a temporal decline, whereas Gammaproteobacteria tended to increase during the mid-exponential phase before declining again by the late exponential stage. This pattern contrasts with Sushmitha et al. (2021), who



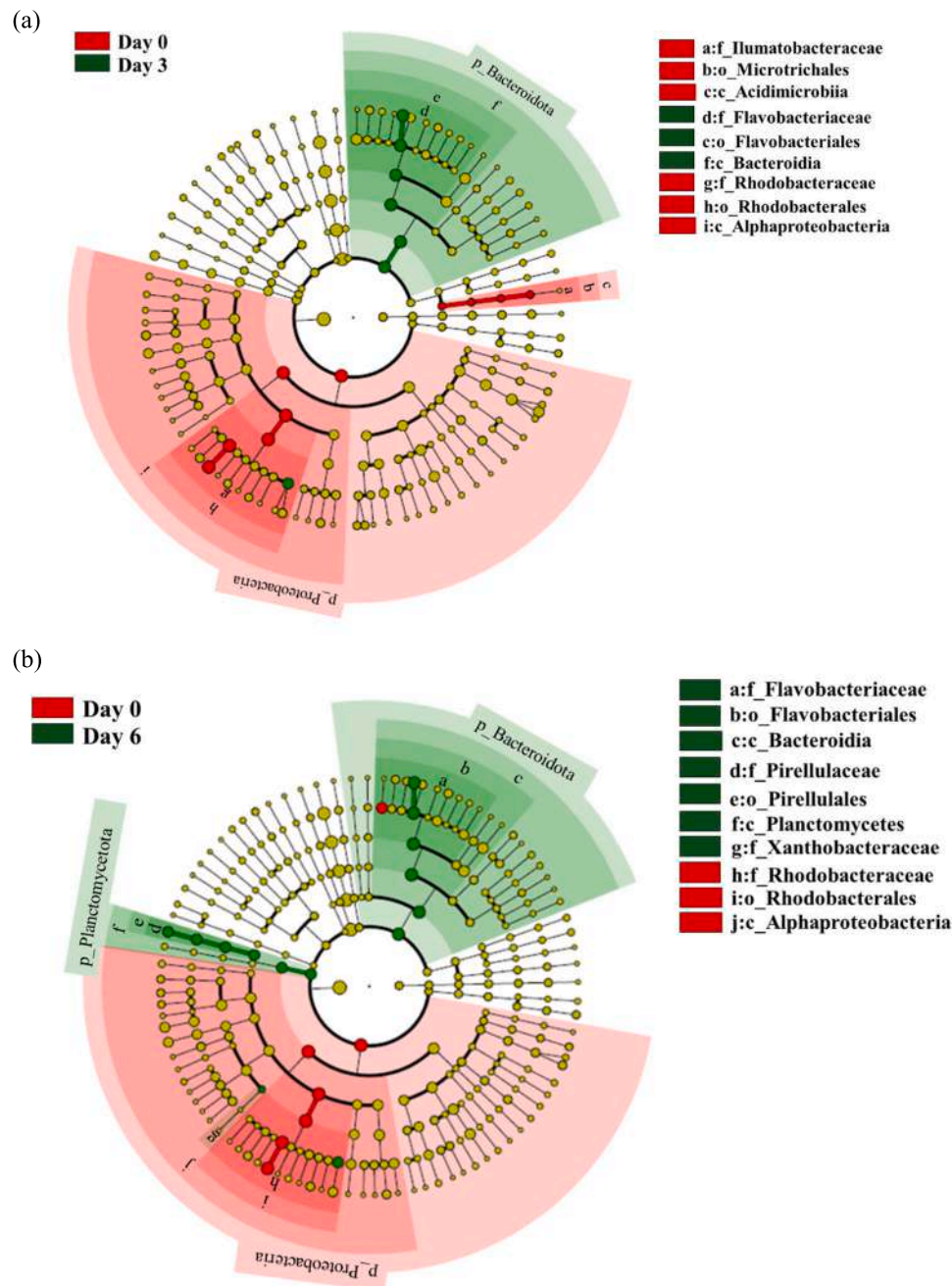


**Fig. 5.** Cladograms to illustrate the temporal succession of bacterial communities associated during the exponential phase of *Amphora* sp. in the biofilm PSBR, sampled at Day 0 (end of pre-incubation of discs), Day 3 (mid-exponential phase), and Day 6 (late-exponential phase) (a) cladogram between Day 0 and Day 3 (b) cladogram between Day 0 and Day 6.  $n = 3$  per harvesting day. In Cladogram, circles radiating from inner side to outer side represent taxonomic rank from phylum to genus (species). Each circle stands for a distinct taxon at corresponding taxonomic rank. The diameter of each circle represents proportionally the relative abundance of each taxon. Coloring principle: Yellow stands for taxons with non-significant differences, Taxons (biomarkers) with significant differences are colored according to corresponding group's color, Red nodes means these microbiota contributes a lot in the group covered by red color, so do the green nodes. The corresponding species of the letters above the circles are annotated on the right side. (For interpretation of the references to color in this figure legend, the reader is referred to the web version of this article.)

identified Gammaproteobacteria as key colonizers in marine biofilms, but agrees with [Dang and Lovell \(2000\)](#), who reported Alphaproteobacteria (Roseobacter) as dominant early colonizers. The mid-exponential rise of Gammaproteobacteria in our study may contribute to ecosystem stabilization, in line with the predicted functional instability of this growth phase, as this group is known to tolerate and thrive under diverse environmental stresses ([Antunes et al., 2020](#)). Within the Bacteroidota phylum, Flavobacteriia was the dominant class, consistent with observations from in situ marine biofilms ([Pollet et al., 2018](#)). Such

shifts imply a successional trajectory influenced by host specificity, geographical variations, seasonal changes, substrate properties, ecological roles, and the availability of resources within the biofilm (particularly the quality and quantity of algal exudates) ([Grossart et al., 2005](#); [Sapp et al., 2007](#); [Pollet et al., 2018](#); [Antunes et al., 2020](#); [Susmitha et al., 2021](#); [Zhang et al., 2024](#)). Collectively, Alphaproteobacteria, Gammaproteobacteria, and Flavobacteriia are known to degrade dissolved and particulate biopolymers such as proteins and polysaccharides ([Sapp et al., 2007](#); [Yoon and Lee, 2012](#); [Xing et al., 2015](#)).

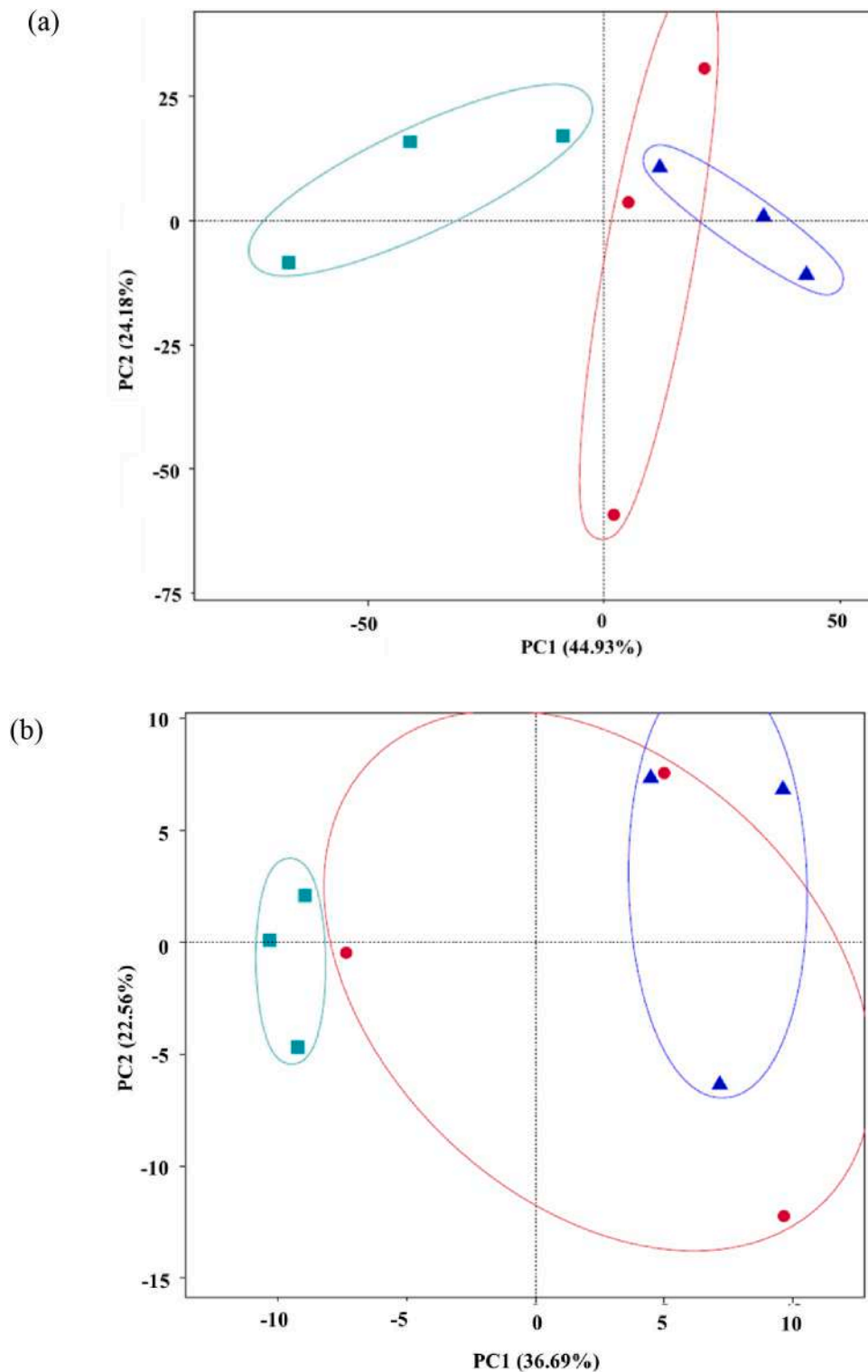


**Fig. 6.** Principal Component Analysis (PCA) of bacterial community functional potential predicted by PICRUSt2, based on (a) Clusters of Orthologous Groups of proteins (COG) and (b) Kyoto Encyclopedia of Genes and Genomes (KEGG) pathway databases. (■) - Day 0 (end of the pre-incubation of discs), (●) - Day 3 (mid-exponential phase), (▲) - Day 6 (late-exponential phase).  $n = 3$  per harvesting day. Functional similarity is indicated by samples clustering close together, whereas differences in functional properties are shown by samples that are farther apart.

At finer taxonomic resolution, several genera emerged as key, phase-associated members of the *Amphora* sp. biofilm. The early dominance of the Roseobacter pioneer *Marivita* (Rhodobacteriaceae, Alphaproteobacteria), is a commonly found bacterial genus in marine environments (Yoon et al., 2013). The higher persistence of this genus as an early

colonizer in the *Amphora* biofilm could likely reflect its versatile metabolic capacity, which includes the uptake and utilization of inorganic and organic carbon, nitrogen, and phosphorus containing compounds, dimethylsulfoniopropionate (DMSP) demethylation, inorganic sulfur oxidation, etc. (Zheng et al., 2019). As observed by Wei et al. (2023) in

planktonic *Phaeodactylum tricornutum* cultures, we also observed a gradual reduction in the abundance of the *Marivita* genus over time, although it remained one of the dominant taxa throughout. This pattern may be attributed to competitive disadvantages as other bacterial groups proliferated and outcompeted it for resources during biofilm maturation. Another versatile genus of the Roseobacter clade, *Sulfitobacter*, maintained a stable presence during the exponential phase of *Amphora* sp. and gradually increased in abundance. This genus is capable of oxidizing reduced sulfur compounds and producing algal growth-promoting metabolites such as indole-3-acetic acid, thereby supporting algal growth and stabilizing diatom-bacteria interactions (Sapp et al., 2007; Amin et al., 2015; Beirlas et al., 2023). Moreover, *Sulfitobacter* can supply ammonia to the diatom in exchange for organosulfur compounds such as taurine and DMSP (Behringer et al., 2018). From the mid-exponential phase onward, *Polaribacter* (Flavobacteriaceae, Flavobacteriia) emerged as the dominant genus, eventually comprising nearly half of the microbial community by the late exponential stage. This successional trajectory is consistent with ecological studies demonstrating that *Polaribacter* thrives during algal blooms in response to the accumulation of diatom-derived polymers such as laminarin, sulfated polysaccharides and other extracellular polysaccharides (Xing et al., 2015; Avcı et al., 2020). In the context of *Amphora* sp. biofilms, this dominance likely reflects similar mechanisms, where *Polaribacter* benefits from the build-up of EPS and other carbon-rich exudates released by the diatom, positioning it as a key player in polymer turnover and biofilm maturation. A late-stage increase of *Rhodopirellula* (Pirellulaceae, Planctomycetota), typically associated with macroalgal biofilms and marine sediments, likely reflects their specialization in degrading complex sulfated polysaccharides and recycling nutrients traits favouring persistence in mature biofilms (Lage and Bondoso, 2012).

Based on PICRUSt2-inferred overall functional potential, both COG analysis (grouping genes into broad functional categories) (Tatusov et al., 2000) and KEGG analysis (linking genes to specific metabolic and regulatory pathways) (Kanehisa and Goto, 2000) revealed that the bacterial community associated with the *Amphora* sp. biofilm had distinct functional profiles across growth phases, with clear differences between the early, with mid, and late exponential stages. Most notably, the mid-exponential phase was characterized by a less stable and more variable profile, whereas the late exponential phase showed functional stabilization. This likely reflects the mid-phase acting as a critical transitional period that precedes the establishment of a stable functional consortium. Such stabilization is crucial for a biofilm to achieve resilience, preserving ecological functions and supporting consistent productivity despite taxonomic turnover. However, functional predictions generated using PICRUSt2 provide only an indirect assessment of the potential metabolic capabilities of the bacterial community, as these predictions are based on phylogenetic inference from 16S rRNA gene data and reference genome databases and are therefore constrained by database coverage, taxonomic resolution, and the assumption that closely related taxa share similar functional repertoires (Langille et al., 2013; Douglas et al., 2020). Moreover, PICRUSt2 does not capture strain-level genomic variation, horizontal gene transfer, or transcriptional regulation, therefore, we interpret the predicted pathways presented here as hypothesis-generating indications of potential functional trends.

As the genera *Marivita*, *Polaribacter*, *Sulfitobacter*, and *Rhodopirellula* were also identified as discriminative biomarkers by LEfSe analysis, bacterial strains from these genera could be promising candidates for forming synthetic consortia, while excluding less abundant genera that could compete for nutrients and space within the biofilm matrix. Their association with *Amphora* during its metabolically active phase highlights their potential for functional interactions without imposing stress on the host, making them suitable for enhancing biofilm resilience, productivity, and scalability in applied systems. We have already shown that *Sulfitobacter* sp. can significantly enhance lipid production of

*Amphora* sp. during the early stages of cultivation in the PSBR. In controlled PSBR co-culture experiments, interactions between *Sulfitobacter* sp. and *Amphora* sp. resulted in an approximately 67% increase in lipid content (dry weight basis), reaching levels up to fivefold higher than those observed in non-axenic *Amphora* sp. cultures and threefold higher than in axenic cultures within a shorter cultivation period (after 3 days) (Gamage et al., 2026b, See Supplementary V for the performance of axenic and non-axenic *Amphora* sp. in the PSBR). Building on these promising findings, the identified genera could be used to design robust and complementary consortia aimed at improving biofilm stability, biomass yield, or lipid productivity of *Amphora* sp. Alternatively, these genera could also serve as candidate model organisms in *Amphora* biofilms for developing quantitative and predictive mathematical models of microalgal-bacterial interactions, as demonstrated by Moejes et al. (2017). Such models not only aid in predicting biofilm productivity and exploring the metabolic potential of microalgae in co-cultures but also play a crucial role in scaling up applications by identifying stable and scalable interactions that ensure consistent performance under applied conditions. While high-throughput sequencing offers major advantages for capturing the broad diversity of bacterial taxa and predicting functions without cultivation (Nwachukwu and Babalola, 2022), it remains limited by primer bias. Many widely used 16S rRNA primers provide suboptimal coverage of prokaryotic communities (Dang and Lovell, 2000; Lupette et al., 2016; Pollet et al., 2018), which can underestimate microbial diversity and mask potentially important interactions. In biofilm studies, where bacterial abundance and distribution are often uneven, such limitations can obscure key players in colonization, succession, or metabolic interactions. In general, optimising culture conditions, increasing replication, and using optimized DNA extraction methods particularly direct extraction rather than filtration can help minimize low-input biases and yield more representative biofilm community profiles. Additionally, metagenomic approaches could also provide a more comprehensive and accurate depiction of community diversity, enabling the reconstruction of bacterial genomes to elucidate their functional potential and dynamics across the diatom's growth phases, which is particularly relevant for microalgal biofilm microbiome engineering studies. Future research should focus on functional analyses of co-cultures between *Amphora* sp. and bacterial strains from the identified genera, including the definition of targeted outcomes (e.g., biomass yield, lipid productivity, biofilm stability, and stress tolerance) and the strategic combination of strains with complementary roles in nutrient cycling and biofilm reinforcement. Furthermore, integrating co-culture experiments with metabolomics and transcriptomics could provide a foundation for engineering stable algal-bacterial biofilms with enhanced resilience, sustained productivity, and targeted applications in microalgal biotechnology.

## 5. Conclusion

This study establishes a foundational framework for screening and selecting suitable native host-associated bacteria for defined algal-bacterial biofilm co-cultures by characterising key bacterial taxa in benthic diatom *Amphora* sp. biofilms during the metabolically active growth period in a PSBR. Distinct phase-dependent shifts in bacterial community composition were observed during the exponential growth phase of *Amphora* sp. cultivated in a PSBR, with a decline in Alphaproteobacteria accompanied by increasing contributions from Flavobacteriia and Planctomycetota. The genera *Marivita*, *Polaribacter*, *Sulfitobacter*, and *Rhodopirellula* emerged as key significant taxa dynamically associated with the exponential growth phase of *Amphora* sp. Bacteria from these genera could be used as candidates for the design of defined synthetic consortia to further explore algal-bacterial interactions in biofilm-based cultivation systems, with the aim of enhancing biofilm resilience and productivity while minimizing the influence of opportunistic or competitive bacteria. In the future, integrating the identified key bacterial taxa into quantitative and predictive



frameworks will not only enable forecasting of biofilm productivity and exploration of *Amphora*'s metabolic potential in co-cultures, but also guide laboratory-based functional studies to optimize biofilm productivity and ensure long-term stability.

### CRedit authorship contribution statement

**Nadeeshani Dehel Gamage:** Writing – original draft, Validation, Methodology, Investigation, Formal analysis, Data curation, Conceptualization. **Paul Deléris:** Writing – review & editing, Writing – original draft, Methodology, Investigation, Formal analysis, Conceptualization. **Leila Tirichine:** Writing – review & editing, Resources, Conceptualization. **Gaëtane Wielgosz-Collin:** Writing – review & editing, Supervision, Methodology, Funding acquisition, Conceptualization. **Thierry Lebeau:** Writing – review & editing, Supervision, Methodology, Investigation, Funding acquisition, Conceptualization. **Aurélien Mossion:** Writing – review & editing, Supervision, Methodology, Conceptualization. **Vona Méléder:** Writing – review & editing, Writing – original draft, Supervision, Resources, Methodology, Investigation, Funding acquisition, Conceptualization.

### Declaration of competing interest

The authors declare that they have no known competing financial interests or personal relationships that could have appeared to influence the work reported in this paper.

### Acknowledgements

We acknowledge financial support from the Région Pays de la Loire (France) through the SMIDAP grant BIOFILM (Agreement No. 2021\_04302), the European Union under the REWRITE project (Grant Agreement 101081357), and the French Ministry of Higher Education, Research and Innovation. We are also grateful to Louis-Josselin Lavier Aydat for his assistance with the Qubit in the US2B laboratory.

### Appendix A. Supplementary data

Supplementary data to this article can be found online at <https://doi.org/10.1016/j.biteb.2026.102686>.

### Data availability

Data will be made available on request.

### References

- Aalto, N.J., Gæver, I.H., Eriksen, G.K., Israelsen, L., Krsmanovic, S., Petters, S., Bernstein, H.C., 2024. The microbiome of bioreactors containing mass-cultivated marine diatoms for industrial carbon capture and utilization. *Algal Res.* 83, 103701. <https://doi.org/10.1016/j.algal.2024.103701>.
- Amin, S.A., Hmelo, L.R., Van Tol, H.M., Durham, B.P., Carlson, L.T., Heal, K.R., Morales, R.L., Berthiaume, C.T., Parker, M.S., Djunaedi, B., Ingalls, A.E., Parsek, M. R., Moran, M.A., Armbrust, E.V., 2015. Interaction and signaling between a cosmopolitan phytoplankton and associated bacteria. *Nature* 522 (7554), 98–101. <https://doi.org/10.1038/nature14488>.
- Antunes, J.T., Sousa, A.A.G., Azevedo, J., Rego, A., Leão, P.N., Vasconcelos, V., 2020. Distinct temporal succession of bacterial communities in early marine biofilms in a Portuguese Atlantic port. *Front. Microbiol.* 11, 1938. <https://doi.org/10.3389/fmicb.2020.01938>.
- Arnaldo, M.D.G., Gamage, N.D., Jaffrenou, A., Rabesaotra, V., Mossion, A., Wielgosz-Collin, G., Méléder, V., 2024. Comparison of different small-scale cultivation methods towards the valorization of a marine benthic diatom strain for lipid production. *Algal Res.* 77, 103327. <https://doi.org/10.1016/j.algal.2023.103327>.
- Avci, B., Krüger, K., Fuchs, B.M., Teeling, H., Amann, R.L., 2020. Polysaccharide niche partitioning of distinct *Polaribacter* clades during North Sea spring algal blooms. *ISME J.* 14 (6), 1369–1383. <https://doi.org/10.1038/s41396-020-0601-y>.
- Behringer, G., Ochsenkühn, M.A., Fei, C., Fanning, J., Koester, J.A., Amin, S.A., 2018. Bacterial communities of diatoms display strong conservation across strains and time. *Front. Microbiol.* 9, 659. <https://doi.org/10.3389/fmicb.2018.00659>.
- Beirlas, R., Ozer, N., Segev, E., 2023. Abundant *Sulfitobacter* marine bacteria protect *Emiliania huxleyi* algae from pathogenic bacteria. *ISME Commun.* 3 (1), 100. <https://doi.org/10.1038/s43705-023-00311-y>.
- Borowitzka, M.A., 2013. High-value products from microalgae: their development and commercialisation. *J. Appl. Phycol.* 25, 743–756. <https://doi.org/10.1007/s10811-013-9983-9>.
- Bui-Xuan, D., Tang, D.Y.Y., Chew, K.W., Nguyen, T.D.P., Ho, H.L., Tran, T.N.T., Nguyen-Sy, T., Dinh, T.H.T., Nguyen, P.S., Dinh, T.M.H., Nguyen, T.T., Shih, P.L., 2022. Green biorefinery: microalgae-bacteria microbiome on tolerance investigations in plants. *J. Biotechnol.* 343, 120–127. <https://doi.org/10.1016/j.jbiotec.2021.12.002>.
- Callahan, B.J., McMurdie, P.J., Holmes, S.P., 2017. Exact sequence variants should replace operational taxonomic units in marker-gene data analysis. *ISME J.* 11, 2639–2643. <https://doi.org/10.1038/ismej.2017.119>.
- Chen, J., Bittinger, K., Charlson, E.S., Hoffmann, C., Lewis, J., Wu, G.D., Collman, R.G., Bushman, F.D., Li, H., 2012. Associating microbiome composition with environmental covariates using generalized UniFrac distances. *Bioinformatics* 28, 2106–2113. <https://doi.org/10.1093/bioinformatics/bts342>.
- Cho, D.H., Ramanan, R., Heo, J., Lee, J., Oh, H.M., Kim, H.M., 2015. Enhancing microalgal biomass productivity by engineering a microalgal-bacterial community. *Bioresour. Technol.* 175, 578–585. <https://doi.org/10.1016/j.biortech.2014.10.159>.
- Chorazyczewski, A.M., Huang, I.S., Abdulla, H., Mayali, X., Zimba, P.V., 2021. The influence of bacteria on the growth, lipid production, and extracellular metabolite accumulation by *Phaeodactylum tricornutum* (Bacillariophyceae). *J. Phycol.* 57 (3), 931–940. <https://doi.org/10.1111/jpy.13132>.
- Cointet, E., Séverin, E., Mossion, A., Méléder, V., Gonçalves, O., Wielgosz-Collin, G., 2021. Assessment of the lipid production potential of six benthic diatom species grown in airlift photobioreactors. *J. Appl. Phycol.* 33 (4), 2093–2103. <https://doi.org/10.1007/s10811-021-02490-4>.
- Dang, H., Lovell, C.R., 2000. Bacterial primary colonization and early succession on surfaces in marine waters as determined by amplified rRNA gene restriction analysis and sequence analysis of 16S rRNA genes. *Appl. Environ. Microbiol.* 66 (2), 467–475. <https://doi.org/10.1128/AEM.66.2.467-475.2000>.
- Davies, F.K., Fricker, A.D., Robins, M.M., Dempster, T.A., McGowen, J., Charania, M., Beliaev, A.S., Lindemann, S.R., Posewitz, M.C., 2021. Microbiota associated with the large-scale outdoor cultivation of the cyanobacterium *Synechococcus* sp. PCC 7002. *Algal Res.* 58, 102382. <https://doi.org/10.1016/j.algal.2021.102382>.
- Dexter, E., Rollwagen-Bollens, G., Bollens, S.M., 2018. The trouble with stress: a flexible method for the evaluation of nonmetric multidimensional scaling. *Limnol. Oceanogr. Methods* 16, 434–443. <https://doi.org/10.1002/lom3.10257>.
- Douglas, G.M., Maffei, V.J., Zaneveld, J.R., Yurgel, S.N., Brown, J.R., Taylor, C.M., Huttenhower, C., Langille, M.C., 2020. PICRUSt2 for prediction of metagenome functions. *Nat. Biotechnol.* 38, 685–688. <https://doi.org/10.1038/s41587-020-0548-6>.
- Filho, M.M.B., Walker, M., Ashworth, M.P., Morris, J.J., 2021. Structure and long-term stability of the microbiome in diverse diatom cultures. *Microbiol. Spectr.* 9, e00269-21. <https://doi.org/10.1128/spectrum.00269-21>.
- Fulbright, S.P., Robbins-Pianka, A., Berg-lyons, D., Knight, R., Reardon, K.F., Chisholm, S.T., 2018. Bacterial community changes in an industrial algae production system. *Algal Res.* 31, 147–156. <https://doi.org/10.1016/j.algal.2017.09.010>.
- Gamage, N.D., Mossion, A., Deléris, P., Delavat, F., Tirichine, L., Rabesaotra, V., Lebeau, T., Wielgosz-Collin, G., Méléder, V., 2026a. Co-culturing with bacteria modulates fatty acid composition in benthic diatom biofilms for lipid-based biotechnologies: a case study of *Amphora* sp. *Algal Res.* 93, 104449. <https://doi.org/10.1016/j.algal.2025.104449>.
- Gamage, N.D., Mossion, A., Khan, M., Karimi, R., Rabesaotra, V., Wielgosz-Collin, G., Lebeau, T., Méléder, V., 2026b. Co-culturing bacteria with monospecific microalgal biofilms for improved biomass and lipid production. *J. Biotechnol.* <https://doi.org/10.1016/j.jbiotec.2026.03.007>.
- Good, I.J., 1953. The population frequencies of species and the estimation of population parameters. *Biometrika* 40, 237–264. <https://doi.org/10.1093/biomet/40.3-4.237>.
- Goto, N., Kawamura, T., Mitamura, O., Terai, H., 1999. Importance of extracellular organic carbon production in the total primary production by tidal-flat diatoms in comparison to phytoplankton. *Mar. Ecol. Prog. Ser.* 190, 289–295. <https://doi.org/10.3354/meps190289>.
- Grossart, H.P., Levold, F., Allgaier, M., Simon, M., Brinkhoff, T., 2005. Marine diatom species harbour distinct bacterial communities. *Environ. Microbiol.* 7, 860–873. <https://doi.org/10.1111/j.1462-2920.2005.00759.x>.
- Indrayani, I., Moheimani, N.R., Boer, K., Bahri, P.A., Borowitzka, M.A., 2020. Temperature and salinity effects on growth and fatty acid composition of a halophilic diatom, *Amphora* sp. MUR258 (Bacillariophyceae). *J. Appl. Phycol.* 32, 977–987. <https://doi.org/10.1007/s10811-020-02053-z>.
- Kanehisa, M., Goto, S., 2000. KEGG: Kyoto Encyclopedia of Genes and Genomes. *Nucleic Acids Res.* 28, 27–30. <https://doi.org/10.1093/nar/28.1.27>.
- Kers, J.G., Saccenti, E., 2022. The power of microbiome studies: some considerations on which alpha and beta metrics to use and how to report results. *Front. Microbiol.* 12, 796025. <https://doi.org/10.3389/fmicb.2021.796025>.
- Krohn-Molt, I., Alawi, M., Förstner, K.U., Wiegandt, A., Burkhardt, L., Indenbirken, D., Thiel, M., Grundhoff, A., Kehr, J., Tholey, A., Streit, W.R., 2017. Insights into microalga and bacteria interactions of selected phycosphere biofilms using metagenomic, transcriptomic, and proteomic approaches. *Front. Microbiol.* 8, 1941. <https://doi.org/10.3389/fmicb.2017.01941>.
- Kumar, G., Shekh, A., Jakhu, S., Sharma, Y., Kapoor, R., Sharma, T.R., 2020. Bioengineering of microalgae: recent advances, perspectives, and regulatory challenges for industrial application. *Front. Bioeng. Biotechnol.* 8, 914. <https://doi.org/10.3389/fbioe.2020.00914>.



- Lage, O.M., Bondoso, J., 2012. Bringing Planctomycetes into pure culture. *Front. Microbiol.* 3, 405. <https://doi.org/10.3389/fmicb.2012.00405>.
- Lakaniemi, A.M., Hulatt, C.J., Wakeman, K.D., Thomas, D.N., Puhakka, J.A., 2012. Eukaryotic and prokaryotic microbial communities during microalgal biomass production. *Bioresour. Technol.* 124, 387–393. <https://doi.org/10.1016/j.biortech.2012.08.048>.
- Langille, M.G.I., Zaneveld, J., Caporaso, J.G., McDonald, D., Knights, D., Reyes, J.A., Clemente, J.C., Burckpile, D.E., Thurber, R.L.V., Knight, R., Beiko, R.G., Huttenhower, C., 2013. Predictive functional profiling of microbial communities using 16S rRNA marker gene sequences. *Nat. Biotechnol.* 31, 814–821. <https://doi.org/10.1038/nbt.2676>.
- Lépinay, A., Turpin, V., Mondegue, F., Grandet-Marchant, Q., Capiaux, H., Baron, R., Lebeau, T., 2018. First insight on interactions between bacteria and the marine diatom *Haslea ostrearia*: algal growth and metabolomic fingerprinting. *Algal Res.* 31, 395–405. <https://doi.org/10.1016/j.algal.2018.02.023>.
- Lian, J., Wijffels, R.H., Smidt, H., Sipkema, D., 2018. The effect of the algal microbiome on industrial production of microalgae. *J. Microbiol. Biotechnol.* 11, 806–818. <https://doi.org/10.1111/1751-7915.13296>.
- Lipsman, V., Shlakhter, O., Rocha, J., Segev, E., 2024. Bacteria contribute exopolysaccharides to an algal-bacterial joint extracellular matrix. *NPJ Biofilms Microbiomes*, 10, 510. <https://doi.org/10.1038/s41522-024-00510-y>.
- Lopes, L.D.B., Soares, R.C., de Freitas, R.M., Amarantem, D.O., de Carvalho, F.C.T., Cavalcante, K.M.S.P., de Sousa, O.V., de Menezes, F.G., 2025. Co-culture of microalgae and bacteria for the production of bioactive compounds. *Ann. Microbiol.* 75, 16. <https://doi.org/10.1186/s13213-025-01804-y>.
- Lozupone, C., Knight, R., 2005. UniFrac: a new phylogenetic method for comparing microbial communities. *Appl. Environ. Microbiol.* 71, 8228–8235. <https://doi.org/10.1128/AEM.71.12.8228-8235.2005>.
- Lozupone, C.A., Knight, R., 2008. Species divergence and the measurement of microbial diversity. *FEMS Microbiol. Rev.* 32 (4), 557–578. <https://doi.org/10.1111/j.1574-6976.2008.00111.x>.
- Lupette, J., Lami, R., Krasovec, M., Grimsley, N., Moreau, H., Piganeau, G., Sanchez-Ferandin, S., 2016. *Marinobacter* dominates the bacterial community of the *Ostreococcus tauri* phycosphere in culture. *Front. Microbiol.* 7, 1414. <https://doi.org/10.3389/fmicb.2016.01414>.
- Moejes, F.W., Succurro, A., Popa, O., Maguire, J., Ebenhö, O., 2017. Dynamics of the bacterial community associated with *Phaeodactylum tricornutum* cultures. *Processes* 5, 77. <https://doi.org/10.3390/pr5040077>.
- Molina-Cárdenas, C.A., Licea-Navarro, A.F., Sánchez-Saavedra, M. del P., 2020. Effects of *Vibrio cholerae* on fatty acid profiles in *Isochrysis galbana*. *Algal Res.* 46, 101802. <https://doi.org/10.1016/j.algal.2020.101802>.
- Nascimento, M.D., Dublan, M.A., Ortiz-Marquez, J.C.F., Curatti, L., 2013. High lipid productivity of an *Ankistrodesmus-Rhizobium* artificial consortium. *Bioresour. Technol.* 146, 400–407. <https://doi.org/10.1016/j.biortech.2013.07.085>.
- Nwachukwu, B.C., Babalola, O.O., 2022. Metagenomics: a tool for exploring key microbiome with the potentials for improving sustainable agriculture. *Front. Sustain. Food Syst.* 6, 886987. <https://doi.org/10.3389/fsufs.2022.886987>.
- Paquette, A.J., Sharp, C.E., Schnurr, P.J., Allen, D.G., Short, S.M., Espie, G.S., 2020. Dynamic changes in community composition of *Scenedesmus*-seeded artificial, engineered microalgal biofilms. *Algal Res.* 46, 101805. <https://doi.org/10.1016/j.algal.2020.101805>.
- Pathom-aree, W., Sattayawat, P., Inwongwan, S., Cheirsilp, B., Liewtrakula, N., Maneechote, W., Rangseekaew, P., Ahmad, F., Mehmood, M.A., Gao, F., Srinuanpan, S., 2024. Microalgae growth promoting bacteria for cultivation strategies: recent updates and progress. *Microbiol. Res.* 286, 127813. <https://doi.org/10.1016/j.micres.2024.127813>.
- Pohl, E., Marxsen, J., Küsel, K., 2010. Pioneering bacterial and algal communities and potential extracellular enzyme activities of stream biofilms. *FEMS Microbiol. Ecol.* 71, 364–373. <https://doi.org/10.1111/j.1574-6941.2009.00817.x>.
- Pollet, T., Berdjeb, L., Garnier, C., Durrieu, G., Le Poupon, C., Misson, B., Briand, J., 2018. Prokaryotic community successions and interactions in marine biofilms: the key role of Flavobacteriia. *FEMS Microbiol. Ecol.* 94, 1–13. <https://doi.org/10.1093/femsec/fiy083>.
- Pushpakumara, B.L.D.U., Tandon, K., Willis, A., Verbruggen, H., 2023. Unravelling microalgal–bacterial interactions in aquatic ecosystems through 16S rRNA gene-based co-occurrence networks. *Sci. Rep.* 13, 2743. <https://doi.org/10.1038/s41598-023-27816-9>.
- Sambrook, J., Russell, D.W., 2001. *Molecular Cloning: A Laboratory Manual*, 3rd ed. vol. 1. Cold Spring Harbor Laboratory Press, New York.
- Sapp, M., Schwaderer, A.S., Wiltshire, K.H., Hoppe, H.G., Gerds, G., Wichels, A., 2007. Species-specific bacterial communities in the phycosphere of microalgae? *Microb. Ecol.* 53, 683–699. <https://doi.org/10.1007/s00248-006-9162-5>.
- Schäfer, H., Abbas, B., Witte, H., Muyzer, G., 2002. Genetic diversity of ‘satellite’ bacteria present in cultures of marine diatoms. *FEMS Microbiol. Ecol.* 42, 25–35. [https://doi.org/10.1016/S0168-6496\(02\)00298-2](https://doi.org/10.1016/S0168-6496(02)00298-2).
- Schmidt, H., Thom, M., Wieprecht, S., Manz, W., Gerbersdorf, S.U., 2018. The effect of light intensity and shear stress on microbial bio-stabilization and the community composition of natural biofilms. *Res Rep Biol.* 9, 1–16. <https://doi.org/10.2147/rb.s145282>.
- Sittmann, J., Bae, M., Mevers, E., Li, M., Quinn, A., Sriram, G., Clardy, J., Liu, Z., 2021. Bacterial diketopiperazines stimulate diatom growth and lipid accumulation. *Plant Physiol.* 186, 1159–1170. <https://doi.org/10.1093/plphys/kiab080>.
- Steinrücken, P., Jackson, S., Müller, O., Puntervoll, P., Kleinegris, D.M.M., 2023. A closer look into the microbiome of microalgal cultures. *Front. Microbiol.* 14, 1108018. <https://doi.org/10.3389/fmicb.2023.1108018>.
- Sushmitha, T.J., Rajeev, M., Murthy, P.S., Ganesh, S., Toleti, S.R., Pandian, S.K., 2021. Bacterial community structure of early-stage biofilms is dictated by temporal succession rather than substrate types in the southern coastal seawater of India. *PloS One* 16, e0257961. <https://doi.org/10.1371/journal.pone.0257961>.
- Tatusov, R.L., Galperin, M.Y., Natale, D.A., Koonin, E.V., 2000. The COG database: a tool for genome-scale analysis of protein functions and evolution. *Nucleic Acids Res.* 28, 33–36. <https://doi.org/10.1093/nar/28.1.33>.
- Vale, F., Sousa, C.A., Simões, L.C., McBain, A.J., Simões, M., 2023. Bacteria and microalgae associations in periphyton-mechanisms and biotechnological opportunities. *FEMS Microbiol. Rev.* 47, 1–23. <https://doi.org/10.1093/femsre/fuad047>.
- Wang, R., Xue, S., Zhang, D., Zhang, Q., Wen, S., Kong, D., Yan, C., Cong, W., 2015. Construction and characteristics of artificial consortia of *Scenedesmus obliquus*–bacteria for *S. obliquus* growth and lipid production. *Algal Res.* 12, 436–445. <https://doi.org/10.1016/j.algal.2015.10.002>.
- Wei, X., Shi, F., Chen, Z., Feng, J., Zhu, L., 2023. Response of bacterial communities (*Marivita*, *Marinobacter*, and *Oceanicaulis*) in the phycosphere to the growth of *Phaeodactylum tricornutum* in different inorganic nitrogen sources. *Front. Mar. Sci.* 10, 1086166. <https://doi.org/10.3389/fmars.2023.1086166>.
- Xing, P., Hahnke, R.L., Unfried, F., Markert, S., Huang, S., Barbeyron, T., Harder, J., Becher, D., Schweder, T., Glöckner, F.O., Amann, R.L., Teeling, H., 2015. Niches of two polysaccharide-degrading *Polaribacter* isolates from the North Sea during a spring diatom bloom. *ISME J.* 9 (6), 1410–1422. <https://doi.org/10.1038/ismej.2014.225>.
- Yoon, J.H., Lee, S.Y., 2012. *Winogradskyella multivorans* sp. nov., a polysaccharide-degrading bacterium isolated from seawater of an oyster farm. *Antonie Van Leeuwenhoek* 102, 231–238. <https://doi.org/10.1007/s10482-012-9729-8>.
- Yoon, J.-H., Kang, S.-J., Lee, J.-S., 2013. *Marivita geojedonensis* sp. nov., isolated from seawater. *Int. J. Syst. Evol. Microbiol.* 63, 423–427. <https://doi.org/10.1099/ijs.0.039065-0>.
- Yuan, H., Wang, Y., Lai, Z., Zhang, X., Jiang, Z., Zhang, X., 2021. Analysing microalgal biofilm structures formed under different light conditions by evaluating cell–cell interactions. *J. Colloid Interface Sci.* 583, 563–570. <https://doi.org/10.1016/j.jcis.2020.09.057>.
- Zhang, L., Chen, F., Zeng, Z., Xu, M., Sun, F., Yang, L., Bi, X., Lin, Y., Gao, Y., Hao, H., Yi, W., Li, M., Xie, Y., 2021. Advances in metagenomics and its application in environmental microorganisms. *Front. Microbiol.* 12, 766364. <https://doi.org/10.3389/fmicb.2021.766364>.
- Zhang, J.-T., Wang, J.-X., Liu, Y., Zhang, Y., Wang, J.-H., Chi, Z.-Y., Kong, F.-T., 2024. Microalgal-bacterial biofilms for wastewater treatment: Operations, performances, mechanisms, and uncertainties. *Sci. Total Environ.* 907, 167974. <https://doi.org/10.1016/j.scitotenv.2023.167974>.
- Zheng, Q., Lu, J., Wang, Y., Jiao, N., 2019. Genomic reconstructions and potential metabolic strategies of generalist and specialist heterotrophic bacteria associated with an estuary *Synechococcus* culture. *FEMS Microbiol. Ecol.* 95, 1–13. <https://doi.org/10.1093/femsec/fiz017>.